

The link between the Star Formation History and $[\alpha/\text{Fe}]$

Ignacio G. de la Rosa^{1,2,3}, Francesco La Barbera⁴, Ignacio Ferreras⁵,
Reinaldo R. de Carvalho⁶

¹ Instituto de Astrofísica de Canarias, C/ Vía Láctea s/n, E-38200 La Laguna, Tenerife, Spain

² Departamento de Astrofísica, Universidad de La Laguna, E-38205 La Laguna, Tenerife, Spain

³ Department of Physics and Astronomy, University College London, Gower Street, London, WC1E 6BT

⁴ INAF - Osservatorio Astronomico di Capodimonte, Napoli, Italy

⁵ Mullard Space Science Laboratory, University College London, Holmbury St Mary, Dorking, Surrey RH5 6NT

⁶ Instituto Nacional de Pesquisas Espaciais/MCT, S.J. dos Campos, Brazil

Accepted for publication in MNRAS Letters, 2011 August 26

ABSTRACT

The abundance ratios between key elements such as iron and α -process elements carry a wealth of information on the star formation history (SFH) of galaxies. So far, simple chemical evolution models have linked $[\alpha/\text{Fe}]$ with the SFH timescale, correlating large abundance ratios with short-lived SFH. The incorporation of full spectral fitting to the analysis of stellar populations allows for a more quantitative constraint between $[\alpha/\text{Fe}]$ and the SFH. In this letter, we provide, for the first time, an empirical correlation between $[\alpha/\text{Fe}]$ (measured from spectral indices) and the SFH (determined via a non-parametric spectral-fitting method). We offer an empirical version of the iconic outline of Thomas et al. (2005, 2010), relating star formation timescale with galaxy mass, although our results suggest, in contrast, a significant population of old ($\gtrsim 10$ Gyr) stars even for the lowest mass ellipticals ($M_s \sim 3 \times 10^{10} M_\odot$). In addition, the abundance ratio is found to be strongly correlated with the time to build up the stellar component, showing that the highest $[\alpha/\text{Fe}]$ ($\gtrsim +0.2$) are attained by galaxies with the shortest half-mass formation time ($\lesssim 2$ Gyr), or equivalently, with the smallest ($\lesssim 40\%$) fraction of populations younger than 10 Gyr. These observational results support the standard hypothesis that star formation incorporates the Fe-enriched interstellar medium into stars, lowering the high abundance ratio of the old populations.

Key words: galaxies: elliptical and lenticular, cD – galaxies: evolution – galaxies: formation – galaxies: stellar content – galaxies: structure.

1 INTRODUCTION

The use of spectral indices has allowed a relatively successful description of the unresolved stellar populations of galaxies in terms of three luminosity-weighted parameters: the age, the global metallicity, and the $[\alpha/\text{Fe}]$ abundance ratio. The advent of new tools of analysis (e.g. spectral fitting), the increasing refinement of the population synthesis models and libraries (e.g. MILES, Sánchez-Blázquez et al. 2006a) and the access to vast spectroscopic surveys (e.g. SDSS, York et al. 2000) allows for a fresh look at well established standards. One of the current paradigms involves the existence of a relationship between $[\alpha/\text{Fe}]$ and the star formation timescale. On the basis of this relationship lies the assumption that the stellar abundance ratios quantify the contribution of different *stellar chronometers* (e.g. supernovae) to the chemical enrichment of the subsequent generations of stars. Core-collapse supernovae, triggered soon after the onset of star formation, release mostly Mg and other α -process elements, whereas type Ia supernovae, with a more complex time delay, contribute large amounts of Fe (see e.g. Greggio & Renzini 1983; Maoz et al.

2011; Mannucci et al. 2005). Hence the $[\alpha/\text{Fe}]$ abundance ratio is a useful tool to track star formation timescales $\Delta t \lesssim 1$ Gyr (see e.g. Matteucci & Tornambé 1987; Thomas et al. 1999; Ferreras & Silk 2003).

By using simple chemical evolution models, Thomas et al. (2005) established a theoretical relationship between the mass of a galaxy and its SFH, described by a Gaussian function. This Gaussian curve is characterized by the mean, given by the SSP-equivalent age, and the FWHM, related to the $[\alpha/\text{Fe}]$ abundance ratios, such that $[\alpha/\text{Fe}] \sim 0.2 - 0.17 \log(\text{FWHM}/\text{Gyr})$. Therefore a high abundance ratio would result from a concentrated burst of star formation, while solar, or sub-solar ratios would reveal a more extended SFH. The application of this rule to observational data by Thomas et al. (2005) and Thomas et al. (2010) produced an iconic outline (figure 9 in Thomas et al. 2010) in which massive galaxies show older and narrower stellar age distributions compared to their less massive counterparts.

There are tools currently available to produce more detailed SFHs than the Gaussian curves described above. The use of spec-

tral fitting (e.g. Cid Fernandes et al. 2005) allows us to probe the full range of populations, giving a more robust estimate of mass-weighted properties. Furthermore, our methodology follows a non-parametric approach, with the goal of establishing a distribution of ages that better maps the spectroscopic data. These estimates are less prone to the biases inherent in the use of luminosity-weighted properties (when using SSPs) or in the parametric assumptions (e.g. when using exponentially decaying SFHs). The analysis of the abundance ratios follows instead the traditional method based on line indices. We emphasize that both properties (SFHs and $[\alpha/\text{Fe}]$ ratios) are therefore extracted independently. In the future, the development of α -enhanced population synthesis models (e.g. Cervantes et al. 2007; Coelho et al. 2007) will open up the possibility of a fully-consistent analysis of the SFHs and the abundance ratios from a spectral fitting point of view ¹

The goal of the present study is to revise the link between the SFH and $[\alpha/\text{Fe}]$ in elliptical galaxies, improving over the insightful outline of Thomas et al. (2005, 2010) by using a combination of *spectral fitting*, to determine non-parametric SFHs, and *line strength* analysis to derive abundance ratios.

2 SAMPLE AND ANALYSIS

Our methodology involves the analysis of the optical spectra to constrain the properties of the underlying stellar populations. The sample is extracted from the $\sim 40,000$ -strong SPIDER catalogue of early-type galaxies (La Barbera et al. 2010) (hereafter Paper I), which covers a redshift range of 0.05 to 0.095 and absolute magnitudes brighter than $M_r = -20$. The spectroscopic data come from the seventh data release (DR7) of the Sloan Digital Sky Survey (SDSS) (Abazajian et al. 2009). We take a subsample with a S/N high enough for a detailed analysis of the stellar populations. We select a set of 9,999 ETGs, belonging to the upper quartile of the distribution in S/N, as measured in the g -band (per-pixel $S/N_g > 18.3$).

Stellar populations are characterized by the following information: **(I)** mass-weighted average ages ($\langle \text{age} \rangle_M$) and metallicities, **(II)** mass-weighted star formation histories (SFHs) and **(III)** average $[\alpha/\text{Fe}]$ abundance ratios. Several techniques and models are available for the extraction of this information. In an ongoing study (de la Rosa et al. in preparation) the performance of several techniques and models has been evaluated for SDSS spectra of similar quality. The methodology chosen for the present study, as described below, results from that performance comparison.

I) Average ages and metallicities are obtained through *spectral fitting* using the STARLIGHT synthesis code (Cid Fernandes et al. 2005) to find the optimal mixture of single stellar populations (SSPs). For the present study, the basis SSPs correspond to 76 solar-scaled MILES models (Vazdekis et al. 2010). These models have a Kroupa Universal Initial Mass Function (Kroupa 2001) and span a range of 4 metallicities, from $Z/Z_\odot=1/50$ to 1.6, and 19 different ages, from 0.5 to 12.6 Gyr. These models are based on the MILES² stellar library (Sánchez-Blázquez et al. 2006a), which combines both a dense coverage of the stellar atmospheric parameters and a relatively high and nearly constant spectral res-

¹ As a robustness check, we have derived galaxy SFHs also with the Cervantes et al. (2007) α -enhanced SSP models, finding good agreement with the results based on the widely used, solar scaled, MILES models.

² www.iac.es/proyecto/miles

Table 1. Uncertainties on Parameters

Parameter	units	typical rms
SFH age-bars	percent	13.4
$\langle \text{age} \rangle_M$	Gyrs	2.7
$\langle [Z/H] \rangle_M$	dex	0.10
$[\alpha/\text{Fe}]$	dex	0.10
$\log(M_{\text{dyn}}/M_\odot)$	dex	0.07

olution (FWHM=2.3Å). The fitting interval spans from 3600 to 7350Å, with emission lines and bad pixels being masked out. The extinction due to foreground dust is modelled with the CCM-law (Cardelli, Clayton & Mathis 1989). The standard output of the spectral fitting consists of the fractional contribution of each SSP to the flux at a normalization wavelength $\lambda_0=4020\text{Å}$, converted into a stellar mass fraction by the M/L of the given SSP at λ_0 , as provided by the models. The detailed population mixture of a galaxy can thus be condensed into a single parameter, the mass-weighted average age, $\langle \text{age} \rangle_M$. The mass-weighted metallicity, $\langle [Z/H] \rangle_M$, is defined in a similar way.

II) The use of *spectral fitting* with solar-scaled MILES models provides the fractional contribution of each SSP to the total flux, allowing for the reconstruction of the SFH. Note that STARLIGHT does not assume any parametric form, describing the SFH by an arbitrary mixture of the basis SSPs. In order to account for the range of redshifts of the sample, we add the corresponding lookback time to the population ages, ranging from 0.67 Gyr ($z=0.05$) to 1.24 Gyr ($z=0.095$). Throughout this paper we assume a standard Λ CDM cosmology with $\Omega_m = 0.3$ and $H_0=70$ km/s/Mpc.

III) The $[\alpha/\text{Fe}]$ is measured with the recent models of Thomas et al. (2011), which provide absorption-line index values for a variety of ages and element abundance ratios. Our procedure fixes the age to its SSP-equivalent value, as obtained from spectral indices $H\beta$ and $[\text{MgFe}]'$. Then, the Mgb and $\text{Fe3} = (\text{Fe4383} + \text{Fe5270} + \text{Fe5335})/3$ indices are compared to the α -enhanced model predictions to obtain the (SSP-equivalent) $[\alpha/\text{Fe}]$. To this effect, all measured indices are preliminarily corrected for both velocity and instrumental dispersion broadening. The correction functions are estimated by convolving a variety of SSP-model spectra with broadening functions of different widths.

Dynamical masses are computed with the formula $M_{\text{dyn},n} = [K(n)R_e\sigma^2]/G$, where n is the Sérsic index and the function $K(n)$ is taken from Bertin et al. (2002). This assumes that mass follows light in a galaxy, and accounts for structural non-homology of galaxy light profiles, as parametrized by the Sersic n . The three relevant parameters, n , R_e and σ , are taken from Paper I.

2.1 Error Estimation

To estimate uncertainties on stellar population parameters, we have resorted to the 2,283 ETGs in the SPIDER sample with repeated spectral observations from the SDSS database (see Paper I). After selecting for pairs of repeated observations with $S/N_g > 18.3$ (i.e. that of the sample used here), a sub-sample of 393 pairs of spectra is explored with the same methodology using differences in the extracted parameters as an estimate of the expected errors. These uncertainties are summarized in table 1. It is worth mentioning that the reported errors refer to single measurements of stellar population parameters, i.e. they reflect the statistical uncertainty inherent in the extraction of SFHs from the noisy spectrum of a

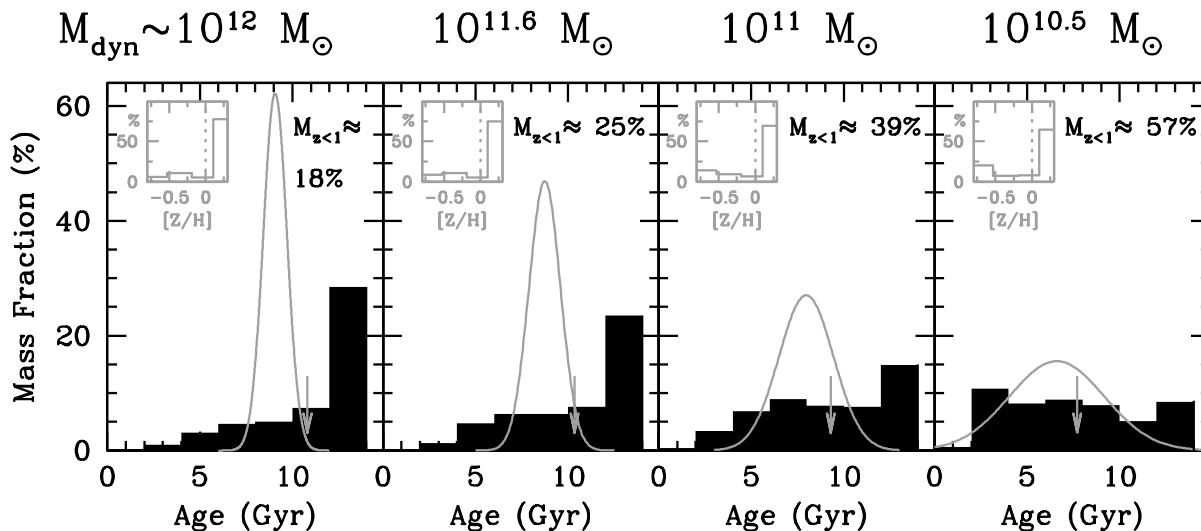


Figure 1. Variation of the star formation history with respect to dynamical mass (each panel representing a mass bin as given in table 2). Sketchy (theoretical) SFHs, plotted as grey Gaussian curves, are superimposed over the detailed (empirical) SFH histograms (black filled) obtained through spectral fitting. The Gaussian curves are obtained from equation 4 of Thomas et al. (2005), using our SSP-equivalent $\langle \text{age} \rangle_L$ (+ lookback time) and $[\alpha/\text{Fe}]$ values, with curves normalized to span the same area as the histograms. Arrows mark the position of the mass-weighted $\langle \text{age} \rangle_M$, obtained from the SFH histograms. Each panel also displays $M_{z<1}$, i.e. the stellar mass percentage formed after $z=1$. The grey insets at the upper-left corners are the metallicity histograms, $([Z/H])_M$, for each mass bin, with a dotted line at the solar metallicity.

Table 2. Stellar population properties as a function of M_{dyn} . For each mass bin, errors on a given quantity are the root-mean-square of deviations from the median value in the bin.

Bin ($\log M_{\text{dyn}}/M_{\odot}$)	12.0	11.6	11.0	10.5
Log Mass interval	11.8 – 12.2	11.5 – 11.7	10.9 – 11.1	10.3 – 10.7
Bin members	1024	1466	1408	690
$\langle \text{age} \rangle_M$ (Gyr)	10.82 ± 1.68	10.35 ± 1.91	9.29 ± 2.22	7.71 ± 2.45
SSP-equiv. age (Gyr)	9.07 ± 2.08	8.74 ± 2.15	7.97 ± 2.47	6.61 ± 2.66
SSP-equiv. $[\alpha/\text{Fe}]$	0.17 ± 0.09	0.15 ± 0.09	0.11 ± 0.09	0.07 ± 0.10

given galaxy. On the other hand, binned quantities in (Figs. 1-2) have much smaller uncertainties, resulting from average-stacking a large sub-sample of galaxies in each bin. The comparison of repeated measurements also shows no systematics in stellar population parameters as a function of S/N, as shown, for σ_0 , in Paper I.

3 RESULTS

3.1 The dependence of SFH with M_{dyn}

Mean SFHs are constructed for four mass bins selected to match the mass intervals of figure 9 in Thomas et al. (2010). Our results for these four mass bins are presented in Table 2, where one can see that the age, metallicity, and abundance ratio parameters actually increase with stellar mass, consistent with previous studies. Figure 1 shows the average distribution of stellar ages for the ETGs within each mass bin. We emphasize that constraints of stellar populations from spectroscopic data are more robust when dealing with *relative* age differences. By constructing a stacked age histogram for all galaxies within each mass bin, we give a rough estimate of

the range of stellar ages to be found in galaxies of the corresponding stellar mass, i.e. an averaged star formation history. Note we use seven time intervals only (instead of the original 19 time steps from the basis SSPs) in order to achieve more robust results (see discussion in Cid Fernandes et al. 2005). The histograms combine all possible metallicities within a given age bin. It is worth mentioning that the absence of the youngest populations ($t \lesssim 2$ Gyr), evident in the depleted left side of the histograms, reflects the limit imposed by the lookback time related to the redshift range of the sample. We do not consider this a problem since most of the stellar populations have ages $\gtrsim 5$ Gyr. Our extracted SFHs (filled black histogram in figure 1) are compared with the ansatz of Thomas et al. (2005, 2010) (grey Gaussian curve), which relate the mean and variance of a Gaussian SFH with the age and $[\alpha/\text{Fe}]$ of the underlying stellar populations. The mean of the Gaussian SFH is set to our SSP-equivalent age with an added lookback time, while the FWHM is extracted from the $[\alpha/\text{Fe}] \sim 0.2 - 0.17 \log(\text{FWHM}/\text{Gyr})$ relation given by Thomas et al. (2005).

We have also constructed stacked metallicity histograms for all galaxies within each mass bin, displaying them as grey insets in figure 1. Histograms show high percentages (60–80 %) of super-

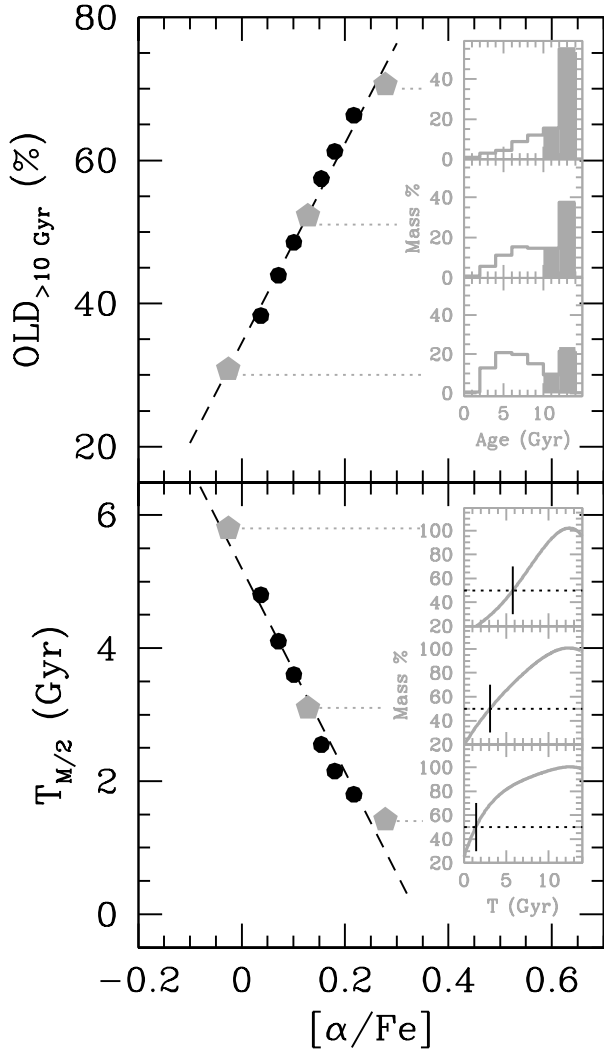


Figure 2. Trends between the SFH and $[\alpha/\text{Fe}]$. The top panel shows the correlation with the mass fraction in old stars ($\gtrsim 10$ Gyr). The insets illustrate individual cases for bins 1, 5 and 9 of the $[\alpha/\text{Fe}]$ distribution (grey pentagons). The shaded histogram bins in the insets mark the $\gtrsim 10$ Gyr populations used for the definition of the OLD parameter. The bottom panel shows the trend with half-mass time (i.e. the time interval over which 1/2 of the total stellar mass is formed). Individual cases of the stellar mass growth for bins 1, 5 and 9 are shown in the insets, with the black lines guiding the eye for the value at 0.5 of total mass.

solar metallicities, with a growing contribution (from 6 to 20 %) of lowest metallicities ($[\text{Z}/\text{H}] < -0.5$) from the highest to the lowest galaxy mass bin. This low metallicity trend might be real, or just reflect the age–metallicity degeneracy and the fact that low- $[\text{Z}/\text{H}]$ stars in the MILES library have super-solar $[\alpha/\text{Fe}]$ (Milone et al. 2011). To test if this can bias our results, we have re-computed the age histograms by excluding galaxies with a significant ($> 20\%$) low $[\text{Z}/\text{H}] (< -0.5)$ population. We found no significant variation *wrt* figure 1 (e.g. less than 1% variation in the SFH for age > 10 Gyr).

A comparison between our SFH extraction and the Gaussian ansatz of Thomas et al. (2005, 2010), shows an overall agreement, although our non-parametric approach gives a more detailed view

of the underlying SFHs. We emphasize that it is the relative difference across mass bins what should be compared and not the absolute age values, whose estimate can be significantly affected by the adopted methodology (e.g. use of spectral-fitting vs. indices) and stellar population libraries. Notice also that the center of the Gaussians does not coincide with that of the SFH histograms, as expected by the fact that luminosity-weighted ages are systematically younger than their mass-weighted counterparts (e.g. Serra & Trager 2007; Rogers et al. 2010). Both the SFH and the Gaussians show the characteristic trend towards younger ages and more extended age distributions in lower mass galaxies.

However, figure 1 goes beyond a simple description of the SFH as a Gaussian. The non-parametric approach of STARLIGHT allows us to study in more detail the relative change of SFHs with respect to galaxy mass. One notices that over the mass range probed, all galaxies feature a significant population of old stars. If we consider the stellar mass formed at redshifts $z > 1$ (i.e. older than ~ 8 Gyr in a local sample) we still get about 40% of stellar mass formed even at $M_{\text{dyn}} \sim 3 \times 10^{10} M_{\odot}$. Furthermore, the most massive galaxies ($M_{\text{dyn}} \sim 10^{12} M_{\odot}$) undergo an intense, short-lived period of star formation, in which over 50% of the stellar mass is formed within a very short period ($\Delta t \lesssim 2$ Gyr) at redshifts $z \gtrsim 4$, followed by a tail of low-level star formation. After $z \sim 1$, only 18% of the stars are newly formed, perhaps the contribution from minor mergers that could explain the size evolution of massive galaxies (see e.g. Naab et al. 2009; Trujillo et al. 2011).

3.2 The dependence of SFH with $[\alpha/\text{Fe}]$

In order to confirm a link between the SFH shape with $[\alpha/\text{Fe}]$, we bin the sample with respect to the abundance ratios into 9 bins, each one containing 1,111 objects. An average SFH is constructed for each bin and two parameters are defined to describe the distribution of stellar ages. The OLD parameter measures the stellar mass fraction contributed by the oldest populations, namely above 10 Gyr. The upper panel of Fig. 2 shows the increase with $[\alpha/\text{Fe}]$ of the OLD parameter. A simple linear regression gives for the mass fraction in old stars:

$$\text{OLD} = 1.397[\alpha/\text{Fe}] + 0.344. \quad (1)$$

For clarity, three insets show the average SFHs for bins 1, 5 and 9 (corresponding to lowest, intermediate, and highest $[\alpha/\text{Fe}]$). The distribution of the extracted values of the OLD parameter for galaxies within the same bin has a standard deviation around 25%. The OLD parameter in these insets corresponds to the added height of the two shaded oldest bins of the histograms. According to this result, the drop in the $[\alpha/\text{Fe}]$ abundance ratio is motivated by a growing fraction of younger populations on top of the prevalent old component. This result supports the standard interpretation (see e.g. Sánchez-Blázquez et al. 2006b), whereby old stellar populations, formed from primeval ingredients, show high $[\alpha/\text{Fe}]$ abundance ratios, further reduced by subsequent star formation episodes, which incorporate the Fe-enriched inter-stellar material into stars.

A complementary view of the same result uses the cumulative integration of the SFH to calculate the “half-mass time” ($T_{M/2}$), i.e. the time needed to form 1/2 of the final stellar mass of the galaxy. We note that the initial time is set to a lookback-time of 13 Gyr for all galaxies. However, this is an arbitrary choice depending on the basis of SSP models used for the *spectral fitting*. The lower panel

of Fig. 2 shows a decreasing $[\alpha/\text{Fe}]$ abundance ratio related to a growing half-mass time $T_{M/2}$, revealing the connection between an extended period of star formation and the decrease of the $[\alpha/\text{Fe}]$ abundance ratio. Similarly to the top panel, the three insets show the average cumulative distribution of the SFH for bins 1, 5 and 9. A simple regression gives:

$$T_{M/2}(\text{Gyr}) = -15.3[\alpha/\text{Fe}] + 5.2, \quad (2)$$

with a scatter around 2.5 Gyr (rms) for galaxies belonging to the same bin in $[\alpha/\text{Fe}]$. The fiducial value for solar abundance ratios is represented, therefore, by a fraction of 34% in stars older than 10 Gyr and a half-mass formation time around 5.2 Gyr.

In general, absolute values of stellar population parameters depend significantly on methods and models used to derive them. Hence, we warn the reader that equations (1) and (2) apply exactly only to the set of models used in the present work, as well as to the lookback time scheme adopted here to bring all SFHs into a common time-frame. In other words, using equations 1 and 2 allows one to convert the $[\alpha/\text{Fe}]$ measured with Thomas et al. (2011) models into half-mass time $T_{M/2}$ and mass fraction in old ($\gtrsim 10$ Gyr) stars, as they would be measured with solar-scaled MILES models and lookback times added up.

4 CONCLUSIONS

This letter presents an independent comparison between the $[\alpha/\text{Fe}]$ abundance ratios and the star formation history of a volume-limited sample of $\sim 10^4$ giant early-type galaxies ($M_r < -20$), extracted from the Sloan Digital Sky Survey. Figure 1 shows the characteristic trend towards more extended SFHs in lower mass ETGs, in agreement with previous work (e.g. Thomas et al. 2005) but with the additional information regarding the distribution of stellar ages. We find that all ETGs in our sample have a significant fraction of very old stars (ages $\gtrsim 10$ Gyr), at variance with the simplified ansatz of a Gaussian SFH of Thomas et al. (2005, 2010). The fraction of stars formed after $z \lesssim 1$ increases from 18% at $M_{\text{dyn}} \sim 10^{12} M_{\odot}$ up to 57% for $M_{\text{dyn}} \sim 3 \times 10^{10} M_{\odot}$. This points to the young populations, formed out of a Fe-enriched medium, as responsible for the decrease of the initially high $[\alpha/\text{Fe}]$ abundance ratios of the old stellar components (see e.g. Sánchez-Blázquez et al. 2006b).

In addition to the SFHs, we used individual absorption lines to determine the $[\alpha/\text{Fe}]$ abundance ratios, following the prescriptions of Thomas et al. (2011). Figure 2 shows the correlation between these two *independently* estimated properties. We find a strong correlation between $[\alpha/\text{Fe}]$ and either the mass fraction in old ($\gtrsim 10$ Gyr) stars (*OLD* parameter; top panel), or the time to form one-half of the current stellar mass of the galaxy ($T_{M/2}$, bottom). Both cases give a clear picture towards enhanced $[\alpha/\text{Fe}]$ for the SFHs that are more short-lived. Those for which $T_{M/2} \lesssim 2$ Gyr feature highest, super-solar, abundance ratios, with $[\alpha/\text{Fe}] \gtrsim 0.2$. Alternatively, an $[\alpha/\text{Fe}] \gtrsim 0.2$ is reached by those galaxies where the old populations ($\gtrsim 10$ Gyr) constitute more than 60% of the stellar mass content. These quantitative results are powerful calibrators of models of galaxy formation.

ACKNOWLEDGMENTS

IGR acknowledges a grant from the Spanish Secretaría General de Universidades of the Ministry of Education, in the frame of its programme to promote the mobility of Spanish researchers to foreign centers. IF acknowledges a grant from the Royal Society and support from the IAC to carry out this research project. We have used data from the SDSS (<http://www.sdss.org/collaboration/credits.html>).

REFERENCES

- Abazajian, K. N., et al. 2009, *ApJS*, 182, 543
 Bertin, G., Ciotti, L., Del Principe, M., 2002, *A&A*, 386, 149
 Cardelli, J. A., Clayton, G. C., Mathis, J. S., 1989, *ApJ*, 345, 245
 Cervantes, J.L., Coelho, P., Barbuy, B., Vazdekis, A., 2007, *Proceedings IAU Symposium No. 241 'Stellar Populations as Building Blocks of Galaxies'*, A. Vazdekis and R.F. Peletier, eds, 167
 Cid Fernandes, R., Mateus, A., Sodré, L., Stasinska, G., Gomes, J. M., 2005, *MNRAS*, 356, 270
 Coelho, P., Bruzual, G., Charlot, S., Weiss, A., Barbuy, B., Ferguson, J.W., 2007, *MNRAS*, 382, 498
 Ferreras, I., Silk, J., 2003, *MNRAS*, 344, 455
 Greggio, L., Renzini, A., 1983, *A&A*, 118, 217
 Kroupa, P. 2001, *MNRAS*, 322, 231
 La Barbera, F., de Carvalho, R. R., de La Rosa, I. G., Lopes, P. A. A., Kohl-Moreira, J. L., Capelato, H. V., 2010, *MNRAS*, 408, 1313 (Paper I)
 Mannucci, F., Della Valle, M., Panagia, N., Cappellaro, E., Cresci, G., Maiolino, R., Petrosian, A., Turatto, M., 2005, *A&A*, 433, 807
 Matteucci, F., Tornambé, F., 1987, *A&A*, 185, 51
 Maoz, D., Mannucci, F., Li, W., Filippenko, A. V., Della Valle, M., Panagia, N., 2011, *MNRAS*, 412, 1508
 Milone, A. de C., Sansom, A.E., Sánchez-Blázquez, P., 2011, *MNRAS*, 414, 1227
 Naab, T., Johansson, P. H., Ostriker, J. P., 2009, *ApJ*, 699, L178
 Rogers, B., Ferreras, I., Peletier, R., Silk, J., 2010, *MNRAS*, 402, 447
 Sánchez-Blázquez, P., Peletier, R. F., Jiménez-Vicente, J., Cardiel, N., Cenarro, A. J., Falcón-Barroso, J., Gorgas, J., Selam, S., Vazdekis, A. 2006, *MNRAS*, 371, 703
 Sánchez-Blázquez, P., Gorgas, J., Cardiel, N., González, J. J., 2006, *A&A*, 457, 787
 Serra P., Trager S. C., 2007, *MNRAS*, 374, 769
 Thomas, D., Greggio, L., Bender, R., 1999, *MNRAS*, 302, 537
 Thomas, D., Maraston, C., Bender, R., Mendes de Oliveira, C., 2005, *ApJ*, 621, 673
 Thomas, D., Maraston, C., Schawinski, K., Sarzi, M., Silk, J., 2010, *MNRAS*, 404, 1775
 Thomas, D., Maraston, C., Johansson, J., 2011, *MNRAS*, 412, 2183
 Trujillo, I., Ferreras, I., de la Rosa, I. G., 2011, *MNRAS*, 415, 3903
 Vazdekis, A., Sánchez-Blázquez, P., Falcón-Barroso, J., Cenarro, J., Beasley, M. A.; Cardiel, N., Gorgas, J., Peletier, R. F. 2010, *MNRAS*, 404, 1639
 York, D. G., et al. 2000, *AJ*, 120, 1579